

## ASSESSMENT OF SENSITIVITY CURVES TO THE IMPROVEMENT OF THE TECHNIQUE OF ESTIMATION OF THERMOPHYSICAL PARAMETERS FROM THERMOGRAPHIES

Alcides Luiz dos Anjos Hora, cidluiz@yahoo.com.br

Fábio Santana Magnani, magnani@ufpe.br

Departamento de Engenharia Mecânica da Universidade Federal de Pernambuco – DEMEC/UFPE  
Av. Acadêmico Hélio Ramos, s/n – 50740-530- Cidade Universitária – Recife – PE – Brasil

**Abstract.** *The thermography as a technique used to extend human vision is still limited in terms of accuracy. The estimation of parameters, moreover, is a technique that requires great precision. In principle it would not be possible to use both techniques simultaneously. However it has been possible to use them provided they use the mean temperature instead of the local temperature. In previous works it was developed a technique where cooling experiments were performed on samples with hidden objects. The results were confronted with simulated ones until the thermophysical parameters could be determined. The aim of the present work is to extend this technique using more samples and performing the assessment of the sensitivity curves in order to obtain greater control over the process. In the cooling experiments the samples are heated until 100 °C and then cooled to room temperature. The experiments are performed on 6 samples: 3 samples with pure materials (steel, plaster or concrete) and 3 samples with hidden objects (steel with the inclusion of a cylinder of plaster, plaster with the inclusion of a cylinder of steel and concrete with the inclusion of a cylinder of brass). For each sample sensitivity curves were determined for thermal conductivity ( $k$ ) and thermal capacity ( $\rho c_p$ ). From the analysis of the curves of sensitivity it was determined the optimum point of the experiment for the estimation of each parameter, which parameters could be or could not be obtained in each case and which parameters could be obtained simultaneously in each case. The proposed extension on the technique allowed both the optimal use and more accurate limits of usage in the estimation of thermophysical parameters from thermographies.*

**Keywords:** *thermography, parameters estimation, sensitivity*

### 1. INTRODUCTION

The major advantage of the use of thermography is the huge number of temperature points that can be measured simultaneously. Its limitation of accuracy (usually  $\pm 2.0^\circ\text{C}$ ) despite the great sensitivity ( $0.08^\circ\text{C}$  in this case) implies the most common usage in qualitative phenomena or in failure detections with rough difference of temperature. Therefore quantitative studies have been made and the usage of infrared camera on quantitative analysis is increasing (Magnani and da Silva, 2007).

Barreira and Freitas (2007), Guerrero et al. (2005) and Al-Kassir et al. (2005) shown cases where infrared imaging could be successfully used. Particularly Dattoma et al. (2001) and Meola et al. (2004) performed studies on the qualitative detection of defects. Determinations of thermal properties are found in Douzane et al. (1999), Venkatesan et al. (2001) and Huang and Tsai (2005).

This work presents a case in which thermographies recorded during a natural convective cooling are used to determine thermophysical characteristics of materials. Six samples are used: three with pure material (steel, plaster and concrete) and three samples with hidden objects (steel with the inclusion of a cylinder of plaster, plaster with the inclusion of a cylinder of steel and concrete with the inclusion of a cylinder of brass) (as shown in Fig. 1). The samples are heated to 100 °C and left to be cooled by natural convection in a 30 °C room. Then the phenomenon is simulated computationally with variable parameters until the deviation between experimental and numerical results is minimized. The whole procedure is divided in three steps: (a) experimental recording of the surface temperature of the samples during the natural cooling, (b) numerical simulation of the pure sample to determine the parameters and (c) numerical simulation of the samples with inclusion to determine the parameters of the inclusion.

The present work is a development of Magnani and da Silva (2007). In this case more samples were manufactured and sensitivity analysis was performed. The use of sensitivity analysis allows the determination of the optimum point to extract the parameters, assess which parameters can be obtained in a specific experiment and which parameters can be obtained simultaneously.

### 2. METHOD

The experiments were performed on six samples: three samples with pure material (steel, plaster and concrete) and three samples with hidden objects (steel with the inclusion of a cylinder of plaster, plaster with the inclusion of a cylinder of steel and concrete with the inclusion of a cylinder of brass). On the posterior discussions samples of pure material are called *pure* followed by the material (e. g., *pure steel*) and samples with inclusion are called *sample with*

*inclusion* (e. g., *sample steel with plaster inclusion*). Pure samples materials were made of steel SAE 1020, a plaster mixture of gypsum and water (1:1 in mass basis) and a concrete mixture with cement, sand and whitewash (1:7:1 in mass basis). For the inclusions the materials used were steel SAE 1020, mixture gypsum and water (1:1 in mass basis) and commercial brass (90% Cu, 10% Al). As discussed in Magnani and da Silva (2007), the mixture of gypsum with water was manipulated and left in a chamber during 4h to homogenize the temperature. The samples of steel (pure and with inclusion) were manufactured by machining. The samples of concrete (pure and with inclusion) were put in a chamber at 50°C for drying during 4 days. According to computational results all the samples were heated at 100°C during 7h to raise and homogenize the temperature.

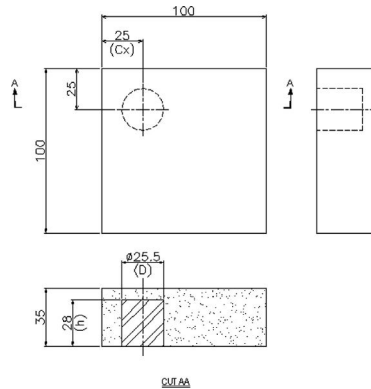


Figure 1– Dimension of sample with inclusion

For the acquisition of the temperature distribution on the surface of the samples it was used an infrared camera model FLIR S45, with 320x240 pixels, frequency of 30 images per second, accuracy of  $\pm 1.0$  °C (calibrated against a blackbody radiation generator with 0.2 °C accuracy), sensibility of 0.08 °C, spectral range of 7.5-13  $\mu\text{m}$  and temperature range of (-40) to 1500 °C. The positioning of the camera in relation to the inclusion is shown in Fig. 2. It should be noticed that the inclusion is hidden from the camera from that position.

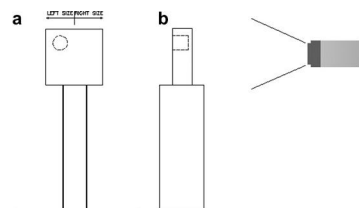


Figure 2– (a) Positioning of the sample over the base, (b) Positioning of the camera in relation with the inclusion.

After the samples were heated to 100 °C they were taken from the chamber with gloved hands and equilibrated over a base formed by two steel plates (1 mm width and 20 cm high). The height was chosen to assure there would be a minimum influence of the base over the natural convection occurring on the samples surfaces (Fig. 2.(a)). The manipulation of the samples took 15 seconds. Experiments showed that the manipulation of the sample do not affects the final thermal behavior of the samples. After the positioning of the sample over the steel base the temperature distribution of the sample surface was recorded on a one minute basis. Figure 3 presents the distribution of temperature of the *sample with inclusion* in three distinct times, in which it is very clear the influence of the inclusion in the surface temperature distribution as the time goes by.

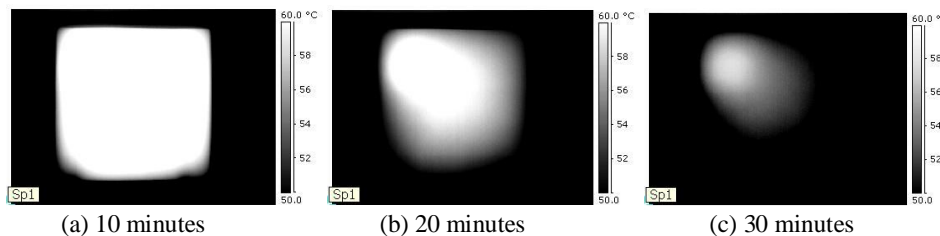


Figure 3 –Evolution of the surface temperature distribution of the plaster *sample with steel inclusion*.

The mean surface temperature is the chosen parameter for the characterization of the thermal behavior of the samples. In order to minimize border effects, it is neglected 5% of each border. The whole process can be summarized on the following steps:

- I) The samples are left to heat and homogenize to 100 °C.
- II) The samples are taken of the chamber and left to cool on a 30 °C atmosphere. During this phenomenon, the mean superficial temperature of the samples was recorded.
- III) Simulations of the cooling of the three pure samples are performed varying the values of the thermal conductivity and thermal capacity (specific mass multiplied by the specific heat) until the simulated curves agree with the experimental ones.
- IV) Simulations of the cooling of the three samples with inclusions are performed varying only the values of the thermal conductivity and thermal capacity of the inclusion. On these simulations, the values of the pure material are the ones determined on step III.
- V) Based on the values estimated on steps III and IV, it is assessed the sensitivity curves of the experiments. 12 curves are constructed, one for each of the 6 materials and 2 parameters (thermal conductivity and capacity).
- VI) For each one of the curves the optimum time is determined. The optimum time is the one in which the sensitivity curve reaches its maximum and consequently the parameter can be estimated with the minimal error.
- VII) New simulations are performed in order to adjust the results on the optimum time. In this way, the parameters roughly estimated on steps III and IV are refined. It should be noticed that the parameters estimated on steps III and IV are used only to determine the optimum time.
- VIII) The parameters are varied until the curves are 1 °C (the camera accuracy) of the experimental data on the optimum time so the error on the parameter estimation can be assessed.

### 3. NUMERICAL SIMULATION

To perform the simulations, the samples are modeled mathematically as parallelepipeds with uniform initial condition (100°C). Each material (pure material and material with inclusion) are modeled with constant and uniform properties. Convection and radiation heat transfer are considered as boundary conditions. The coefficients of convection are determined using distinct classical empirical correlations (Kreith, 2000) for the vertical, upper horizontal and lower horizontal surfaces. To take into account the movement of the samples from the stove to the steel plate base the coefficient of convection in the beginning of the simulation is majored tenfold. It was tested in the simulations that this increase on the coefficient of convection in the very beginning of the simulation has no effect on the final temperature distribution, because the great resistance for heat loss is the conduction in the interior of the sample and not the natural convection on the surface. The mathematical model is discretized using the finite volumes method, in a regular and uniform grid, using the fully implicit method for the time discretization. In each time step, the new coefficients of natural convection are calculated based on the surface distribution of temperature. Various grid sizes were tested: (a) Spatial sizes:  $6 \cdot 6 \cdot 6 \cdot 200$ ,  $10 \cdot 10 \cdot 10 \cdot 200$ ,  $16 \cdot 16 \cdot 16 \cdot 200$ ,  $20 \cdot 20 \cdot 20 \cdot 200$ ,  $26 \cdot 26 \cdot 26 \cdot 200$ ,  $30 \cdot 30 \cdot 30 \cdot 200$  and (b) Time sizes:  $20 \cdot 20 \cdot 20 \cdot 200$ ,  $20 \cdot 20 \cdot 20 \cdot 150$  and  $20 \cdot 20 \cdot 20 \cdot 200$ . For both the three first numbers stand for number of elements on the spatial dimensions and the last stands for the number of time steps. The results were confronted for spatial size and time size. The best grid size was determined once the next result was approximately equal to the last one. Throughout this work the  $20 \cdot 20 \cdot 20 \cdot 200$  was the used grid.

### 4. RESULTS DISCUSSION

The following discussion is guided by the steps described in section 2. Figures 4-6 show the experimental superficial mean temperature obtained during the natural cooling of the 6 samples. First of all it can be seen that all the samples have the expected decay of temperature. One important set of results is the comparison between the temperature of the pure samples and the ones with the inclusions. Figure 5 shows the difference of 3.3 °C reached in the experiments with the sample of pure plaster and the sample of plaster with a steel inclusion. The high thermal capacity of the steel forces a higher superficial temperature. The concrete/brass pair of samples (Fig. 6) qualitatively shows the same behavior of the plasterboard/steel pair (Fig. 5), but quantitatively presents a lower temperature difference of 2 °C. Although brass and steel have thermal capacity in the same magnitude, the higher conductivity of the concrete in relation with the plasterboard minimizes the effect of the inclusion. Figure 4 shows the difference between the temperature of the pure steel sample and the sample of steel with a plasterboard inclusion. In this case the high conductivity of the steel and the lower heat capacity of the plasterboard of the inclusion make the effect of the inclusion almost imperceptible.

The results of steps III and IV are also presented in Figs. 4-6 where it can be seen the adjustment of the simulated results with the experimental ones. As it was said in the third section the very beginning of the phenomenon is simulated considering a tenfold convection rate. This was the way used to consider the handy manipulation of the samples.

It can be seen in Figs. 4-6 that the results obtained with this corrections present a good adjustment in the phenomenon as a whole. First of all the thermal conductivity and capacity of the pure samples were determined in order to adjust the simulated curves with the experimental data. With those results the thermal conductivity and capacity of the inclusions were determined. It should be stressed that once the difference between the mean superficial temperature of the sample of pure steel and the sample of steel with a plaster inclusion was small it was not possible to estimate the parameters of the steel inclusion.

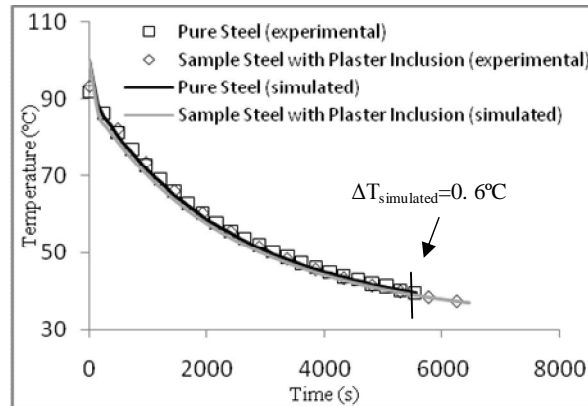


Figure 4. Comparison between experimental and simulated mean surface temperature evolution of *sample steel* (pure and with inclusion)

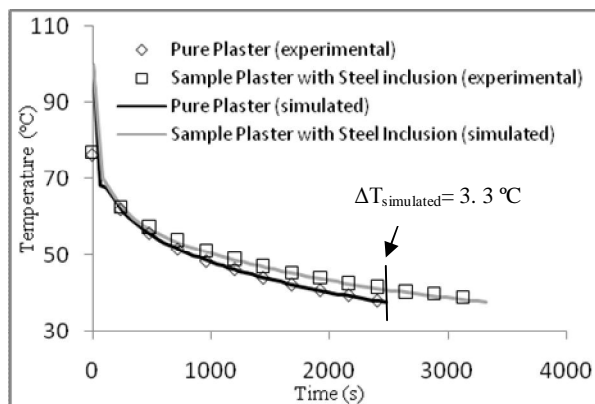


Figure 5. Comparison between experimental and simulated mean surface temperature evolution of *sample plaster* (pure and with inclusion)

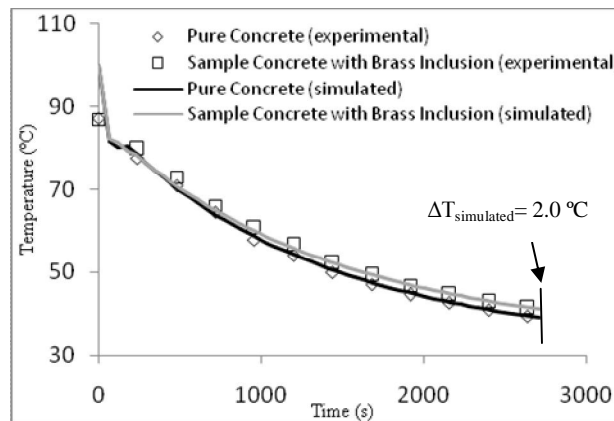


Figure 6. Comparison between experimental and simulated mean surface temperature evolution of *sample concrete* (pure and with inclusion)

After the estimation of the thermal conductivity and thermal capacity of the 3 parallelepipeds (steel, plaster and concrete) and 3 cylindrical inclusions (steel, plaster, and brass) it was performed the sensitivity analysis of the phenomenon. In this way the results obtained in steps III and IV are not the conclusive ones but used only as and primary estimation to perform the sensitivity analysis.

$$S(x,r) = \frac{dx}{dr} \cdot \frac{r}{x} \tag{1}$$

where:

$S(x,r)$  – sensitivity of  $x$  to  $r$   
 $x$  and  $r$  -generic variables

Equation 1 presents the definition of the sensitivity of  $x$  to  $r$ . The meaning of this quantity is the impact on a percentage basis of the parameter  $r$  on the  $x$  variable. For example if  $S(x,r)$  has a value of 3 it means that a 1% of variation on the parameter  $r$  implies on a 3% variation on the variable  $x$ . When used for parameter estimation usually  $x$  is the measured variable (temperature in this case) and  $r$  is the parameter to be estimated (thermal conductivity and thermal capacity in this case). The accuracy of the parameter will be the percentual error of the temperature sensor (1 °C) divided by the value of  $S(r,x)$  as can be seen by equations 2 and 3. So the greater the value of  $S(x,r)$  the lower the error on the estimated parameter.

$$\frac{d(\rho c_p)}{\rho c_p} = \frac{dT}{T} \cdot \frac{1}{S(T, \rho c_p)} \tag{2}$$

where:

$S(T, \rho c_p)$  - sensitivity of  $T$  to  $\rho c_p$   
 $T$  – mean surface temperature [°C]  
 $\rho c_p$  - thermal capacity (specific mass multiplied by the specific heat) [ J/m<sup>3</sup>K]

$$\frac{d(k)}{k} = \frac{dT}{T} \cdot \frac{1}{S(T, k)} \tag{3}$$

where:

$S(T, k)$  - sensitivity of  $T$  to  $k$   
 $k$  - thermal conductivity [w/mK]

Another important information in the  $S(x,r)$  is the ability of the method to estimate more than one parameter simultaneously. Following Beck et al. (1985) the simultaneously estimation is possible when the  $S(x,r)$  curves for the parameters are not linearly dependent.

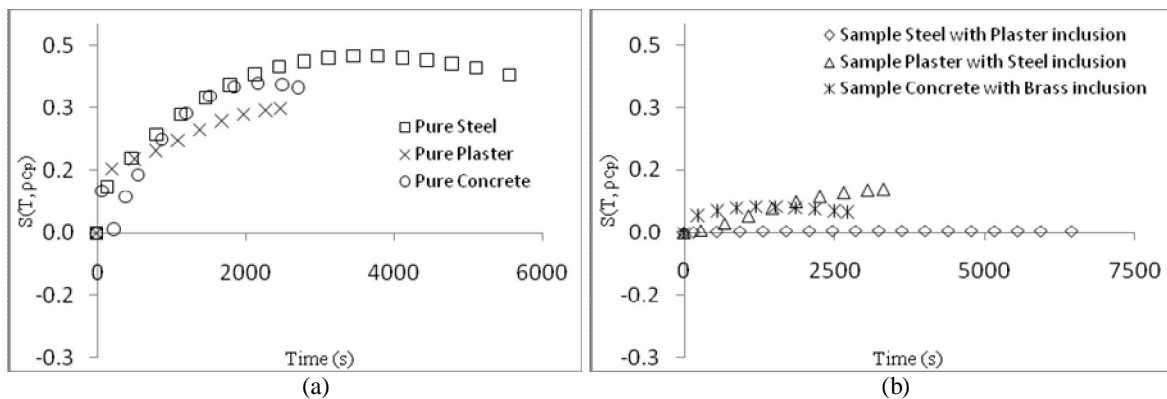


Figure 7. Evolution of sensitivity  $S(T, \rho c_p)$  for (a) pure sample and (b) the inclusion.

Figure 7(a) presents the results for the sensibility of the mean superficial temperature of the 3 pure samples in respect to the thermal capacity of the parallelepiped. It can be seen that the values of  $S(x,r)$  are higher than 0.25 in the

maximum of the curves. Figure 7(b) shows the results for the sensitivity for the 3 inclusions. In that case the values of the sensitivity are lower. One should notice the very low value of the sensitivity for the steel inclusion in all the experiment. This explains the impossibility to estimate the value of the thermal capacity in step IV.

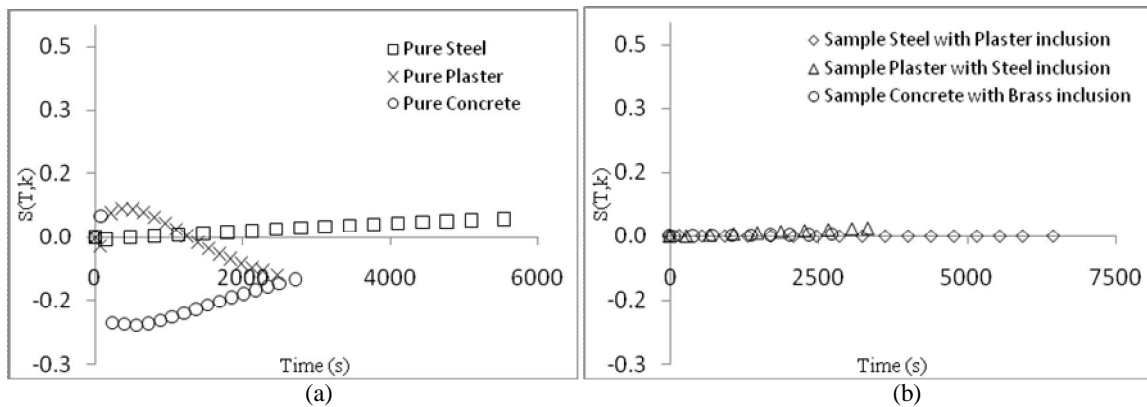


Figure 8. Evolution of sensitivity  $S(T, k)$  for (a) pure sample and (b) the inclusion.

Figure 8(a) and 8(b) present the analogous results of figures 7(a) and 7(b) but for the thermal conductivity. It can be noticed that the sensitivity of the heat conductivity for the pure steel is somewhat low. This occurs probably because in this case the high conductivity transfers the great thermal resistance to the natural convection. Although this was not performed in this work it can be expected that the steel sample would be the best for the estimation of the coefficient of convection. The values for the sensitivity of the 3 inclusions were low as shown in figure 8(b). This explains the high error obtained on these values.

Based on the results of the  $S(x, r)$  curves it was possible to determine the best time for the parameter estimation. Those values can be seen on Tabs. 1-3. For example, the best time to estimate the thermal capacity of the steel parallelepiped is 3560s as can be seen on Fig. 7(a). The value of the parameters on the best time were estimated by varying those values until the values of both simulated and experimental temperature on the best time vanished. The value of the error for each parameter were estimated by varying the parameters until the temperature difference reached 1°C (sensor accuracy).

Table 1. Results of the determination of parameters for Steel sample pair.

Parameters	Pure Steel		Sample Steel with Plaster Inclusion	
	Thermal Conductivity	Thermal Capacity	Thermal Conductivity of plaster inclusion	Thermal Capacity of plaster inclusion
$S(x, r)^{(1)}$	0.043	0.425	-	-
$t^{(1)}$	5548(s)	3560(s)	-	-
Found Value	$35 \pm 20$ (w/mK) 57.14%	$3471060 \pm 167280$ (J/m <sup>3</sup> K) 4.82%	-	-

<sup>(1)</sup>: Found value in the best time

As already discussed the greater the sensitivity the lower the parameter error. This can be seen systematically in Tabs. 1-3. It should be stressed that the parameter error was not obtained by equation 1 but as explained on the previous paragraph. Further studies are necessary to understand when the values of the error obtained by both ways should be equal.

Table 2. Results of the determination of parameters for Plaster sample pair.

Parameters	Pure Plaster		Sample Plaster with Steel Inclusion	
	Thermal Conductivity	Thermal Capacity	Thermal Conductivity of steel inclusion	Thermal Capacity of steel inclusion
$S(x, r)^{(1)}$	-0.089	0.297	0.018	0.105
$t^{(1)}$	2472(s)	2472(s)	3317(s)	3317(s)
Found Value	$0.055 \pm 0.017$ (w/mK) 30.91%	$669120 \pm 58548$ (J/m <sup>3</sup> K) 8.75%	$80 \pm 115$ (w/mK) 143.75%	$2509200 \pm 669120$ (J/m <sup>3</sup> K) 26.67%

<sup>(1)</sup>: Found value in the best time

Table 3. Results of the determination of parameters for Concrete sample pair.

Parameters	Pure Concrete		Sample Concrete with Brass Inclusion	
	Thermal Conductivity	Thermal Capacity	Thermal Conductivity of brass inclusion	Thermal Capacity of brass inclusion
$S(x,r)^{(1)}$	-0.208	0.361	0.004	0.064
$t^{(1)}$	500(s)	2228(s)	2714(s)	1364(s)
Found Value	$1.55 \pm 0.5$ (w/mK) 32.26%	$1633000 \pm 15000$ (J/m <sup>3</sup> K) 0.92%	$45 \pm 265$ (w/mK) 588.9%	$3200000 \pm 920000$ (J/m <sup>3</sup> K) 28.75%

<sup>(1)</sup>: Found value in the best time

## 5. SUMMARY AND CONCLUSION

This work is an extension and improvement of Magnani and da Silva (2007). It was used more samples: 3 pairs of materials instead of only 1. The use of more samples permitted the confirmation that the method can be used on same pairs but not the others. For example, the high conductivity of the steel transferred the comparatively higher thermal resistance for the convection so raising the error of the parameters of the steel.

The improvement was performed by the sensitivity analysis absent in the previous work. Knowing what is the best moment to estimate the parameter has two advantages: minimizing the error because of the greater sensibility and avoiding the performance of the experiment beyond the best time.

Further research will be directed to new experiments focusing on the repeatability of the experiments, exploitation of Eq. (1) for the error estimation, estimation of other parameter as coefficient of convection and geometry of the inclusion. Additionally it will be performed an investigation on the relation between the number of points used on the mean temperature and the error on the parameter. This investigation is very important on the use of simpler infrared cameras on the parameter estimation.

## 6. ACKNOWLEDGEMENTS

The authors would like to acknowledge FINEP and CNPq.

## 7. REFERENCES

- Al-Kassir, A.R., Fernandez, J., Tinaut, F.V. and Castro, F., 2005, "Thermographic study of energetic installations", *Applied Thermal Engineering*, Vol. 25, pp. 183–190.
- Barreira, E., Freitas, V.P., 2007, "Evaluation of building materials using infrared thermography", *Construction and Building Materials*, Vol. 21, pp. 218-224.
- Beck, J.V., Blackwell, B., St. Clair, Jr, C.R., "Inverse Heat Conduction – III-posed Problems", Willey-Interscience, 1985.
- Dattoma, V., Marcuccio, R., Pappalettere, C., Smith, G.M., 2001, "Thermographic investigation of sandwich structure made of composite material", *NDT&E International*, Vol. 34, pp. 515–520.
- Douzane, O., Roucoult, J.M., Langlet, T., 1999, "Thermophysical property measurements of building materials in a periodic state", *International Journal of Heat and Mass Transfer*, Vol. 42, pp. 3943–3958.
- Guerrero, I.C., Ocaña, S.M., Requena, I.G., 2005, "Thermal–physical aspects of materials used for the construction of rural buildings in Soria (Spain)", *Construction and Building Materials*, Vol. 19, pp 197–211.
- Huang, C.-H., Tsai, Y.-L., 2005, "A transient 3-D inverse problem in imaging the time-dependent local heat transfer coefficients for plate fin", *Applied Thermal Engineering*, Vol. 25, pp 2478–2495.
- Kreith, F., 2000, "The CRC Handbook of Thermal Engineering", CRC Press, Boca Raton.
- Magnani, F. S., Da Silva, R. N. T., 2007, "Infrared thermography applied to the quantitative determination of spatial and thermophysical parameters of hidden included objects", *Applied Thermal Engineering*, Vol. 27, pp. 2378–2384.
- Meola, C., Carlomagno G.M., Giorleo, L., 2004, "The use of infrared thermography for materials characterization", *Journal of Materials Processing Technology*, Vol. 155–156, pp. 1132–1137.
- Venkatesan, G., Jin, G.-P., Chyu, M.-C., Zheng, J.-X., Chu, T.-Y., 2001, "Measurement of thermophysical properties of polyurethane foam insulation during transient heating", *International Journal of Thermal Sciences*, Vol. 40, pp 133–144.

## 8. RESPONSIBILITY NOTICE

The authors are the only responsible for the printed material included in this paper.